A New Tripodal Iron(III) Monophenolate Complex: Effects of Ligand Basicity, Steric Hindrance, and Solvent on Regioselective Extradiol Cleavage

Ramasamy Mayilmurugan,[†] Eringathodi Suresh,[‡] and Mallayan Palaniandavar*,[†]

School of Chemistry, Bharathidasan University, Tiruchirapalli 620 024, India, and Analytical Science Discipline, Central Salt and Marine Chemicals Research Institute, Bhavnagar 364 002, India

Received April 4, 2007

The new iron(III) complex [Fe(L3)Cl_2], where H(L3) is the tripodal monophenolate ligand *N,N*-dimethyl-*N*′-(pyrid-2-ylmethyl)-*N*′-(2-hydroxy-3,5-dimethylbenzyl)ethylenediamine, has been isolated and studied as a structural and functional model for catechol dioxygenase enzymes. The complex possesses a distorted octahedral iron(III) coordination geometry constituted by the phenolate oxygen, pyridine nitrogen and two amine nitrogens of the tetradentate ligand, and two cis-coordinated chloride ions. The Fe–O–C bond angle (134.0°) and Fe–O bond length (1.889 Å) are very close to those (Fe–O–C, 133° and 148°, Fe–O(tyrosinate), 1.81 and 1.91 Å) of protocatechuate 3,4-dioxygenase enzymes. When the complex is treated with $AgNO_3$, the ligand-to-metal charge transfer (LMCT) band around 650 nm (ϵ, 2390 M^{-1} cm^{-1}) is red shifted to 665 nm with an increase in absorptivity (ϵ, 2630 M^{-1} cm^{-1}) and the Fe^{III}/Fe^{II} redox couple is shifted to a slightly more positive potential (–0.329 to –0.276 V), suggesting an increase in the Lewis acidity of the iron(III) center upon the removal of coordinated chloride ions. Furthermore, when 3,5-di-*tert*-butylcatechol (H_2DBC) pretreated with 2 mol of Et_3N is added to the complex [Fe(L3)Cl_2] treated with 2 equiv of $AgNO_3$, two intense catecholate-to-iron(III) LMCT bands (719 nm, ϵ, 3150 M^{-1} cm^{-1}; 494 nm, ϵ, 3510 M^{-1} cm^{-1}) are observed. Similar observations are made when H_2DBC pretreated with 2 mol of piperidine is added to [Fe(L3)Cl_2], suggesting the formation of [Fe(L3)(DBC)] with bidentate coordination of DBC^{2-}. On the other hand, when H_2DBC pretreated with 2 mol of Et_3N is added to [Fe(L3)Cl_2], only one catecholate-to-iron(III) LMCT band (617 nm; ϵ, 4380 M^{-1} cm^{-1}) is observed, revealing the formation of [Fe(L3)(HDBC)(Cl)] involving monodentate coordination of the catecholate. The appearance of the DBSQ/H_2DBC couple for [Fe(L3)-(DBC)] at a potential (–0.083 V) more positive than that (–0.125 V) for [Fe(L3)(HDBC)(Cl)] reveals that chelated DBC^{2-} in the former is stabilized toward oxidation more than the coordinated $HDBC^{-}$. It is remarkable that the complex [Fe(L3)(HDBC)(Cl)] undergoes slow selective extradiol cleavage (17.3%) of H_2DBC in the presence of O_2, unlike the iron(III)–phenolate complexes known to yield only intradiol products. It is probable that the weakly coordinated (2.310 Å) –NMe_2 group rather than chloride in the substrate-bound complex is displaced, facilitating O_2 attack on the iron(III) center and, hence, the extradiol cleavage. In contrast, when the cleavage reaction was performed in the presence of a stronger base-like piperidine before and after the removal of the coordinated chloride ions, a faster intradiol cleavage was favored over extradiol cleavage, suggesting the importance of the bidentate coordination of the catecholate substrate in facilitating intradiol cleavage. Also, intradiol cleavage is favored in dimethylformamide and acetonitrile solvents, with enhanced intradiol cleavage yields of 94 and 40%, respectively.

Introduction

The aerobic degradation of aromatic compounds typically proceeds via a catecholic intermediate that is cleaved into a product[1] with the incorporation of molecular oxygen. The ring cleavage reactions are catalyzed by two classes of dioxygenases, distinguished on the basis of regiospecificity: the intradiol dioxygenases cleave the C−C bond between the hydroxyl groups of catechol on coordination to the non-

* To whom correspondence should be addressed. E-mail: palani51@sify.com or palanim51@yahoo.com.
[†] Bharathidasan University.
[‡] Central Salt and Marine Chemicals Research Institute.

(1) (a) Que, L., Jr. In *Bioinorganic Catalysis*, 2nd ed.; Reedijk, J., Ed.; Marcel Dekker: New York, 1993; pp 347−393. (b) Kruger, H.-J. *Biomimetic Oxidations Catalyzed by Transition Metal Complexes*; Meunier, B., Ed.; Imperial College Press: London, 2000; pp 363−413.

Scheme 1. Structures of Sterically hindered Mono- and Bisphenolate Ligands

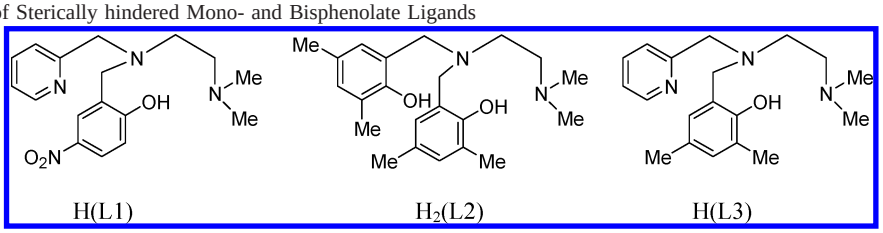

heme iron(III) center[2−14] by a novel substrate activation mechanism,[2] while the extradiol dioxygenases generally utilize non-heme iron(II) to cleave the C−C bond adjacent to hydroxyl groups through an oxygen activation mechanism.[3] The X-ray crystal structure of the intradiol-cleaving protocatechuate 3,4-dioxygenase (3,4-PCD) from *Pseudomonas putida* reveals a trigonal-bipyramidal iron(III) site with four endogenous protein ligands (Tyr408, Tyr447, His460, and His462) and a solvent-derived ligand.[4−9,15] Furthermore, recent crystallographic and spectral studies have shown that upon bidentate coordination of a catecholate substrate[10,11] the axial Tyr447 residue and the equatorial hydroxide are displaced from the iron(III) center, inducing the iron active-site geometry to alter from trigonal-bipyramidal to square-pyramidal. In contrast to intradiol dioxygenases, extradiol dioxygenases contain iron(II) ligated to two histidines, a glutamate ligand, and two water molecules in the active site, forming a square-pyramidal coordination geometry.[13−15] Also, they represent the more common cleavage pathway, but insight into these enzymes has lagged behind that of intradiol-cleaving enzymes.[13]

Mimicking the function of dioxygenases through the synthesis and study of small molecule active-site analogues can provide useful data to improve our understanding of structure−function correlations for the protein metal sites. In earlier studies, several biomimetic iron complexes were constructed as structural and functional models for catechol dioxygenases.[12,13,16−25] Several structurally well-defined octahedral iron(III) complexes[12,13,16−25] were reacted with 3,5-di-*tert*-butylcatechol (H_2DBC) in the presence of O_2 to afford intradiol cleavage products. The ligand-donor functionalities in them exhibit different stereoelectronic effects in influencing the Lewis acidity of the iron(III) center and hence its catalytic intradiol cleavage activity. Very recently, we have observed[20] that the incorporation of a sterically hindering $-NMe_2$ group in the iron(III)−phenolate complex [Fe(L1)Cl_2] (**1**), where H(L1) is *N*,*N*-dimethyl-*N*′-(pyrid-2-ylmethyl)-*N*′-(2-hydroxy-4-nitrobenzyl)ethylenediamine (Scheme 1), imposes a relatively high Fe−O−C bond angle of 136.1°. Furthermore, interestingly, the incorporation of two 3,5-dimethylphenolate arms in the iron(III)−phenolate complex [Fe(L2)Cl] (**2**), where H_2(L2) is *N*,*N*-dimethyl-*N*′,*N*′-bis(2-hydroxy-3,5-dimethylbenzyl)ethylenediamine (Scheme 1), confers a trigonal-bipyramidal coordination geometry on iron(III),[19] but the complex fails to elicit catechol dioxygenase activity. In the present study, we have extended our work on iron(III) complexes of sterically hindered ligands to understand the effect of incorporating only one 3,5-dimethylphenolate arm, as in [Fe(L3)Cl_2] (**3**), where H(L3) is *N*,*N*-dimethyl-*N*′-(2-hydroxy-3,5-dimethylbenzyl)-*N*′-(pyrid-2-ylmethyl)ethylenediamine (Scheme 1). The H_2DBC binds in a monodentate mode to iron(III) in this octahedral complex despite having two cis-coordinated chloride ions, and it is cleaved regiospecifically to yield extradiol-cleavage products in major quantities and intradiol-cleavage products in smaller quantities. This is interesting, because to date, only a few

(2) Que, L., Jr.; Lipscomb, J. D.; Munck, E.; Wood, J. M. *Biochim. Biophys. Acta* **1977**, *485*, 60−74.
(3) (a) Que, L., Jr. In *Iron Carriers and Iron Proteins*; Loehr, T. M., Ed.; VCH: New York, 1989; pp 467−524. (b) Shu, L.; Chiou, Y.-M.; Miller, A. M.; Lipscomb, J. D.; Que., L., Jr. *Biochemistry* **1995**, *34*, 6649−6659.
(4) Ohlendorf, D. H.; Lipscomb, J. D.; Weber, P. C. *Nature* **1988**, *336*, 403−405.
(5) Ohlendorf, D. H.; Orville, A. M.; Lipscomb, J. D. *J. Mol. Biol*. **1994**, *244*, 586−608.
(6) Valley, M. P.; Brown, C. K.; Burk, D. L.; Vetting, M. W.; Ohlendorf, D. H.; Lipscomb, J. D. *Biochemistry* **2005**, *44*, 11024−11039.
(7) Frazee, R. W.; Orville, A. M.; Dolbeare, K. B.; Yu, H.; Ohlendorf, D. H.; Lipscomb, J. D. *Biochemistry* **1998**, *37*, 2131−2144.
(8) (a) Vetting, M. W.; D'Argenio, D. A.; Ornston, L. N.; Ohlendorf, D. H. *Biochemistry* **2000**, *39*, 7943−7955. (b) Elgren, T. E.; Orville, A. M.; Kelly, K. A.; Lipscomb, J. D.; Ohlendorf, D. H.; Que, L., Jr. *Biochemistry* **1997**, *36*, 11504−11513.
(9) Vetting, M. W.; Ohlendorf, D. H. *Structure* **2000**, *8*, 429−440.
(10) (a) Whittaker, J. W.; Lipscomb, J. D.; Kent, T. A.; Munck, E.; Orme-Johnson, N. R.; Orme-Johnson, W. H. *J. Biol. Chem*. **1984**, *259*, 4487−4495. (b) Orville, A. M.; Lipscomb, J. D. *J. Biol. Chem*. **1989**, *264*, 8791−8801. (c) True, A. E.; Orville, A. M.; Pearce, L. L.; Lipscomb, J. D.; Que, L., Jr. *Biochemistry* **1990**, *29*, 10847−10854.
(11) (a) Orville, A. M.; Lipscomb, J. D.; Ohlendorf, D. H. *Biochemistry* **1997**, *36*, 10052−10066. (b) Orville, A. M.; Elango, N.; Lipscomb, J. D.; Ohlendorf, D. H. *Biochemistry* **1997**, *36*, 10039−10051.
(12) (a) Lauffer, R. B.; Heistand, R. H., II; Que, L., Jr. *J. Am. Chem. Soc*. **1981**, *103*, 3947−3949. (b) Heistand, R. H., II; Roe, A. L.; Que, L., Jr. *Inorg. Chem*. **1982**, *21*, 676−681. (c) Heistand, R. H., II; Lauffer, R. B.; Fikrig, E.; Que, L., Jr. *J. Am. Chem. Soc*. **1982**, *104*, 2789−2796. (d) Lauffer, R. B.; Heistand, R. H., II; Que, L., Jr. *Inorg. Chem*. **1983**, *22*, 50−55. (e) White, L. S.; Nilsson, P. V.; Pignolet, L. H.; Que, L., Jr. *J. Am. Chem. Soc*. **1984**, *106*, 8312−8313. (f) Pyrz, J. W.; Roe, A. L.; Stern, L. J.; Que, L., Jr. *J. Am. Chem. Soc*. **1985**, *107*, 614−620. (g) Que, L., Jr.; Kolanczyk, R. C.; White, L. S. *J. Am. Chem. Soc*. **1987**, *109*, 5373−5380. (h) Funabiki, T.; Sakamoto, H.; Yoshida, S.; Tarama, K. *J. Chem. Soc., Chem. Commun*. **1979**, 754-755. (i) Funabiki, T.; Yamazaki, T.; Fukui, A.; Tanaka, T.; Yoshida, S. *Angew. Chem., Int. Ed*. **1998**, *37*, 513−515. (j) Ogo, S.; Yamahara, R.; Funabiki, T.; Masuda, H.; Watanabe, Y. *Chem. Lett*. **2001**, 1062−1063. (k) Funabiki, T.; Fukui, A.; Hitomi, Y.; Higuchi, M.; Yamamoto, T.; Tanaka, T.; Tani, F.; Naruta, Y. *J. Inorg. Biochem*. **2002**, *91*, 151−158. (l) Funabiki, T.; Sugio, D.; Inui, N.; Maeda, M.; Hitomi, Y. *Chem. Commun*. **2002**, 412−413. (m) Hitomi, Y.; Higuchi, M.; Tanaka, T.; Funabiki, T. *Inorg. Chim. Acta* **2005**, *358*, 3465−3470. (n) Higuchi, M.; Hitomi, Y.; Minami, H.; Tanaka, T.; Funabiki, T. *Inorg. Chem*. **2005**, *44*, 8810−8821. (o) Lim, J. H.; Lee, H.-J.; Lee, K.-B.; Jang, H. G. *Bull. Korean Chem. Soc*. **1997**, *18*, 1166−1171.
(13) (a) Que, L., Jr.; Ho, R. Y. N. *Chem. Rev*. **1996**, *96*, 2607−2624. (b) Costas, M.; Mehn, M. P.; Jensen, M. P.; Que, L., Jr. *Chem. Rev*. **2004**, *104*, 939−986.
(14) Abu-Omar, M.; Loaiza, A.; Hontzeas, N. *Chem. Rev*. **2005**, *105*, 2227−2252.
(15) Davies, M. I.; Orville, A. M.; Neese, F.; Zaleski, J. M.; Lipscomb, J. D.; Solomon, E. I. *J. Am. Chem. Soc*. **2002**, *124*, 602−614.
(16) Yamahara, R.; Ogo, S.; Masuda, H.; Watanabe, Y. *J. Inorg. Biochem*. **2002**, *88*, 284- 294.
(17) Jang, H. G.; Cox, D. D.; Que, L., Jr. *J. Am. Chem. Soc*. **1991**, *113*, 9200−9204.

synthetic iron(III) model complexes have been reported to serve as functional models for extradiol-cleaving catechol dioxygenases. Funabiki et al. found that $FeCl_2/FeCl_3$ with pyridine/bipyridine in THF/H_2O cleaves H_2DBC to produce extradiol products in 40% yield.[26] The complex [Fe^{III}(TACN)(DBC)(Cl)], in which TACN (1,4,9-triazacyclononane) is cis-facially coordinated, afforded[27] the extradiol product (2-pyrone, 35%) upon exposure to O_2, and removal of the coordinated chloride ion in the complex provides an almost quantitative yield[28] of the extradiol-cleavage product. Iron(III) complexes of certain cis-facially coordinating tridentate ligands[29] elicited extradiol cleavage up to 97% (pyrone) and also the complex [$Fe^{III}(Tp^{i-Pr_2})$(DBC)],[30] where Tp^{i-Pr_2} is the cis-facially coordinating tripodal ligand hydridotris(3,5-diisopropyl-1-pyrazolyl)borate, gave major amounts of extradiol-cleavage products (2-pyrone). The iron(III) 4N ligand complexes [Fe(6-Me_3−TPA)(DBC)]$^+$, where 6-Me_3−TPA = tris(6-methylpyrid-2-ylmethyl)amine, and [Fe(BLPA)(HDBC)]$^{2+}$, where BLPA = bis((6-methylpyrid-2-ylmethyl)-(pyrid-2-yl-methyl)amine, and [Fe(6-Me_2−BPMCN)(DBC)]$^+$, where 6-Me_2−BPMCN = *N*,*N*′-dimethyl-*N*,*N*′-bis(6-methylpyrid-2-ylmethyl)-1,2-cyclohexadiamine, elicited measurable amounts of extradiol-cleavage products (3, 20, and 12%, respectively).[31] Also, both Fe^{III} and Fe^{II} complexes of a variety of macrocyclic ligands yielded the authentic extradiol product 2-hydroxymuconic semialdehyde.[32] Thus, the iron(III) complex [Fe(L−N_4H_2)(DBC)]$^+$, where L−N_4H_2 = 2,11-diaza[3,3](2,6)pyridinophane, reacts with O_2 to afford a roughly 1:1 mixture of extradiol- and intradiol-cleavage products.[33] Furthermore, no iron(III)−phenolate complex has been shown so far to yield extradiol-cleavage products, and so observation of the present iron(III)−phenolate complex **3** yielding regioselective extradiol-cleavage products is remarkable. However, intradiol-cleavage products have been obtained in higher quantities on removal of the coordinated chloride ions in **3** in methanol and exclusively in dimethylformamide (DMF) and CH_3CN solvents.

Experimental Section

Materials. *N*,*N*-Dimethylethylenediamine, 3,4,5,6-tetrachlorocatechol (H_2TCC, Lancaster), 3,5-di-*tert*-butylcatechol (H_2DBC), 4-*tert*-butylcatechol (H_2TBC), 2,4-dimethylphenol, 2-pyridinecarboxaldehyde, catechol (H_2CAT), 4-nitrocatechol (H_2NCAT, Aldrich), iron(III) chloride (anhydrous) (Merck, India), 3-methylcatechol (3-H_2MCAT), and 4-methylcatechol (4-H_2MCAT) (Acros Organics) were used as received, unless noted otherwise, and H_2-DBC was recrystallized from hexane before use. The supporting electrolyte tetrabutylammonium perchlorate (NBu_4ClO_4, G. F. Smith, USA) was recrystallized twice from aqueous ethanol.

Physical Measurements. Elemental analyses were performed on a Perkin-Elmer Series II CHNS/O Analyzer 2400. ^{1}H NMR spectra were recorded on a Bruker 200 MHz NMR spectrometer. The electronic spectra were recorded on Varian Cary 300 double-beam UV−vis and Agilent 8453 diode array UV−vis spectrophotometers. The EPR spectra were recorded on a JEOL JES-TE 100 X-band spectrometer. Cyclic voltammetry (CV) and differential pulse voltammetry (DPV) were performed using a three-electrode cell configuration. A platinum sphere, a platinum plate, and Ag(s)/Ag^+were used as working, auxiliary, and reference electrodes, respectively. The supporting electrolyte used was NBu_4ClO_4 (TBAP). The temperature of the electrochemical cell was maintained at 25 ± 0.2 °C by a cryocirculator (HAAKE D8 G). By the bubbling of research-grade nitrogen, the solutions were deoxygenated and an atmosphere of nitrogen was maintained over the solutions during measurements. The $E_{1/2}$ values were observed under identical conditions for various scan rates. The instruments utilized included an EG&G PAR 273 potentiostat/galvanostat and a Pentium-IV computer along with EG&G M270 software to carry out the experiments and to acquire the data. The product analyses were performed using a HP 6890 GC series gas chromatograph equipped with a flame ionization detector (FID) and an HP-5 capillary column (30 m × 0.32 mm × 2.5 μm), and the GC-MS analysis was performed on a Perkin-Elmer Clarus 500 GC-MS instrument using a PE-5 with the previously[20] reported temperature program.

Synthesis of Ligand. *N*,*N*-Dimethyl-*N*′-(pyrid-2-ylmethyl)-*N*′-(2-hydroxy-3,5-dimethylbenzyl)ethylenediamine (H(L3)). The ligand H(L3) was synthesized in two steps. The first step in the synthesis was the preparation of *N*,*N*-dimethyl-*N*′-(pyrid-2-ylmethyl)ethylenediamine, which was then reacted with 2,4-dimethylphenol and 37% formalin solution in the second step to obtain H(L3).

Step 1. *N*,*N*-Dimethyl-*N*′-(pyrid-2-ylmethyl)ethylenediamine was prepared as reported[19] elsewhere. ^{1}H NMR (200 MHz, $CDCl_3$): δ 2.20 (s, $N(CH_3)_2$), 2.4 (t, CH_2), 2.7 (t, CH_2), 3.90 (s, py−CH_2), 3.0 (sb, NH), 7.1−8.5 (pyH).

Step 2. *N*,*N*-Dimethyl-*N*′-(pyrid-2-ylmethyl)ethylenediamine (1.94 g, 10.8 mmol) was added to 37% formalin (1.22 g, 16.2 mmol) in

(18) (a) Viswanathan, R.; Palaniandavar, M. *J. Chem. Soc., Dalton Trans*. **1995**,1259−1266. (b) Viswanathan, R.; Palaniandavar, M.; Balasubramanian, T.; Muthiah, P. T. *Inorg. Chem*. **1998**, *37*, 2943−2951. (c) Dhanalakshmi, T.; Bhuvaneshwari, M.; Palaniandavar, M. *J. Inorg. Biochem*. **2006**, *100*, 1527−1534. (d) Palaniandavar, M.; Velusamy, M.; Mayilmurugan, R. *J. Chem. Sci. (Bangalore, India)* **2006**, *118*, 601−610. (e) Palaniandavar, M.; Mayilmurugan, R. *C. R. Chim*. **2007**, *10*, 366−379.

(19) Velusamy, M.; Palaniandavar, M.; Srinivasa Gopalan, R.; Kulkarni, G. U. *Inorg. Chem*. **2003**, *42*, 8283−8293.

(20) Velusamy, M.; Mayilmurugan, R.; Palaniandavar, M. *Inorg. Chem*. **2004**, *43*, 6284−6293.

(21) Velusamy, M.; Mayilmurugan, R.; Palaniandavar, M. *J. Inorg. Biochem*. **2005**, *99*, 1032−1042.

(22) (a) Pascaly, M.; Duda, M.; Rompel, A.; Sift, B. H.; Klaucke, an, W. M.; Krebs, B. *Inorg. Chim. Acta* **1999**, *291*, 289−299. (b) Pascaly, M.; Nazikkol, C.; Scweppe, F.; Wiedeman, A.; Zurlinden, K.; Muller.; Krebs, B. *Z. Anorg. Allg. Chem*. **2000**, *626*, 50−55. (c) Duda, M.; Pascaly, M.; Krebs, B. *J. Chem. Soc., Chem. Commun*. **1997**, 835−836. (d) Merkel, M.; Baldeau, S. M; Schindlers, D.; Krebs, B. *Inorg. Chem*. **2005**, *44*, 7582−7589. (e) Merkel, M.; Pascaly, M.; Krebs, B.; Astner, J.; Foxon, S. P.; Schindler, S. *Inorg. Chem*. **2005**, *44*, 7582−7589.

(23) Merkel, M.; Müller, F. K.; Krebs, B. *Inorg. Chim. Acta* **2002**, *337*, 308−316.

(24) Pascaly, M.; Duda, M.; Schweppe, F.; Zurlinden, F.; Muller, K.; Krebs, B. *J. Chem. Soc., Dalton Trans*. **2001**, 828−837.

(25) Koch, W. O.; Krüger, H.-J. *Angew. Chem., Int. Ed. Engl*. **1995**, *34*, 2671−2674.

(26) (a) Funabiki, T.; Mizoguchi, A.; Sugimoto, T.; Tada, S.; Tsuji, M.; Sakamoto, H.; Yoshida, S. *J. Am. Chem. Soc*. **1986**, *108*, 2921−2932. (b) Funabiki, T.; Mizoguchi, A.; Sugimoto, T.; Yoshida, S. *Chem. Lett*. **1983**, 917−920.

(27) Die, A.; Gatteschi, D.; Pardi, L. *Inorg. Chem*. **1993**, *32*, 1389−1395.

(28) Ito, M.; Que. L., Jr. *Angew. Chem., Int. Ed*. **1997**, *36*, 1342−1344.

(29) Jo, D.-H.; Que. L., Jr. *Angew. Chem., Int. Ed*. **2000**, *39*, 4284−4287.

(30) Oghihara, T.; Hikichi, S.; Akita, M.; Moro-oka, Y.; *Inorg. Chem*. **1998**, *37*, 2614−2615.

(31) Jo, D.-H.; Chiuo, Y.-M.; Que. L., Jr. *Inorg. Chem*. **2001**, *40*, 3181−3190.

(32) (a) Lin, G.; Reid, G.; Bugg, T. D. H. *Chem. Commun*. **2000**, 1119−1120. (b) Lin, G.; Reid, G.; Bugg, T. D. H. *J. Am. Chem. Soc*. **2001**, *123*, 5030−5039.

(33) Raffard, N.; Carina, R.; Simaan, A. J.; Sainton, J.; Riviere, E.; Tchertanov, L.; Bourcier, S.; Bouchoux, G.; Delroisse, M.; Banse, F.; Girerd, J.-J. *Eur. J. Inorg. Chem*. **2001**, 2249−2254.

methanol (10 mL) at 0 °C under nitrogen, and then 2,4-dimethylphenol (1.32 g, 10.8 mmol) in methanol (8 mL) was added to this dropwise. The solution was allowed to warm to room temperature and then treated with acetic acid (3 mL). After the mixture was stirred for 48 h, the solvent was removed under vacuum, neutralized with dilute NaOH, and extracted three times with CH_2C1_2. The organic layer was dried over Na_2SO_4, and CH_2C1_2 was removed under vacuum to get the ligand H(L3). The crude product was then purified by passing it over a silica column using CH_2C1_2 as the eluent. The yield was 60% as a viscous oil. ^{1}H NMR (200 MHz, $CDCl_3$): δ 2.25 (s, 6H, CH_3), 2.35 (s, 6H, N−CH_3), 2.55 (s, 4H, CH_2CH_2), 3.55 (s, 2H, Ph−CH_2), 3.70 (s, py−CH_2), 6.60, 6.75 (s, aryl), 7.05−7.9 (s, py−H).

Syntheses of Complexes. The complex [Fe(L3)Cl_2] (**3**) was prepared by the reaction of a solution of ferric chloride (0.16 g, 1.0 mmol) in methanol (5 mL) to a methanolic solution (10 mL) of an equivalent amount of the ligand H(L3) (0.31 g, 1.0 mmol) in the presence of an equivalent amount of triethylamine (Et_3N) (0.10 g, 140 μL, 1.0 mmol) in stoichiometric combination. The solution was stirred and then refluxed for an hour. The blue-colored precipitate obtained was filtered off, washed with small amounts of cold methanol, and dried in vacuo over P_4O_{10}. The yield was 0.33 g (75%). Anal. Calcd. for $C_{19}H_{26}N_3OFeCl_2$: C, 51.96; H, 5.97; N, 9.57. Found: C, 51.91; H, 6.01; N, 9.64. X-ray quality crystals were obtained by the slow evaporation of a methanolic solution of the complex. The complex [Fe(L2)Cl] (**2**) was prepared by using the reported procedure.[19]

Kinetics and Product Analysis. The kinetic analysis[17,19−25,34] of the catechol-cleavage reactions was carried out by a time-dependent measurement of the disappearance of the lower-energy catecholate-to-iron(III) ligand-to-metal charge transfer (LMCT) band at ambient temperature (25 °C) by exposing the catecholate adducts generated in situ to molecular oxygen. The solvents were equilibrated at the atmospheric pressure of O_2 at 25 °C, and the solubility of O_2 at 25 °C is as follows: methanol, 2.12×10^{-3} M;[24,35] acetonitrile, 8.1×10^{-3} M;[25,35] and DMF,[19,20,35] 4.86×10^{-3} M. A stock solution of the adduct [Fe(L3)(HDBC)(Cl)][33,36] was prepared by treating the complex **3** (1.0×10^{-2} M) with an equivalent amount of H_2DBC pretreated with 2 equiv of Et_3N. The adduct [Fe(L3)(DBC)] was generated in situ by treating **3** (1.0×10^{-2} M) with an equivalent amount of H_2DBC pretreated with 2 equiv of piperidine. The adduct [Fe(L3)(DBC)] was generated in methanol in situ also by treating **3** (1.0×10^{-2} M) with 2 equiv of $AgNO_3$, centrifuging the solution to remove AgCl, and then adding to it 1 equiv of H_2DBC pretreated with 2 equiv of Et_3N. The adduct [Fe(L3)(DBC)] was generated in acetonitrile or DMF in situ by treating **3** (1.0×10^{-2} M) with an equivalent amount of H_2DBC pretreated with 2 equiv of Et_3N. Oxygenation was started by rapid delivery of a stock solution (0.1 mL) of the catecholate adducts (1.0×10^{-2} M) by syringe to O_2-saturated solvent (4.9 mL).

The products of dioxygenation of catecholate adducts of **3** were determined by using a known[20,26,37,38] procedure with modifications. The complex **3** (44 mg, 0.1 mmol), H_2DBC (22 mg, 0.1 mmol), and Et_3N (20 mg, 28 μL, 0.2 mmol) or piperidine (17 mg, 20 μL, 0.2 mmol) were dissolved in methanol/DMF/CH_3CN (10 mL) and stirred under an oxygen atmosphere. For reactions in methanol, DMF, and CH_3CN, piperidine was used as the base. After 24 (piperidine) or 48 h (Et_3N), the oxygenation reaction was quenched by the addition of 6 M HCl solution (25 mL). The products were extracted from the aqueous solution with $CHCl_3$ (3×50 mL). The clear yellow $CHCl_3$ layer was separated, washed twice, first with 2 M HCl (20 mL) and then with water, and then extracted with a saturated $NaHCO_3$ solution (10 mL) to separate the acid products. The $CHCl_3$ layer was saved for further manipulation to obtain nonacid products. The aqueous solution was acidified with 6 M HCl and then extracted twice with 5 mL of $CHCl_3$. The $CHCl_3$ extracts were combined, dried over anhydrous Na_2SO_4, filtered, and the solvent was rotaevaporated to yield an acid product. The $CHCl_3$ layer remaining after $NaHCO_3$ extraction was dried over 5 g of anhydrous Na_2SO_4 at room temperature. The Na_2SO_4 was then filtered off, rinsed twice with 5 mL of fresh $CHCl_3$, and the combined filtrate was evaporated in vacuo at 40 °C, which yields nonacid products. Further purification of the products was accomplished by column chromatography using silica gel and 200 mL of $CHCl_3$ as eluent. The major products were separated and dissolved in $CDCl_3$ and analyzed by GC, GC-MS, and ^{1}H NMR techniques. The other minor products were analyzed as a mixture, detected by GC-MS (EI) (EI = electron ionization), and quantified using GC (FID) with the following temperature program: initial temperature, 50 °C; heating rate 5 °C min^{-1}; final temperature 250 °C; injector temperature 150 °C; and FID temperature 280 °C. GC-MS analysis was performed under conditions identical to those used for GC analysis.

cis,cis-3,5-Di-*tert*-butyl-2-hydroxymuconic semialdehyde (**9**). GC-MS (EI) data found for $C_{14}H_{20}O_4$: *m*/*z* 252. ^{1}H NMR (200 MHz, $CDCl_3$): δ 1.10 (s, 9H), 1.17 (s, 9H), 5.90 (s, 1H), 9.85 (s, 1H). The ^{1}H NMR data were in agreement with literature data.[26,32,37,38]

3,5-Di-*tert*-butyl-5-(2-oxo-2-piperidinylethyl)-5*H*-furanone (**7**). GC-MS (EI) data found for $C_{19}H_{31}NO_3$: *m*/*z* 321. ^{1}H NMR (200 MHz, $CDCl_3$): δ 1.10 (s, 9H), 1.21 (s, 9H), 1.54 (m, 6H), 2.90 and 3.06 (2H), 3.40 (m, 4H), 7.14 (s, 1H). The GC-MS and ^{1}H NMR data were in agreement with literature data.[12e,20,21]

Single-Crystal X-ray Data Collection and Structure Solution. A crystal of suitable size was selected from the mother liquor, immersed in paraffin oil, mounted on the tip of a glass fiber, and cemented using epoxy resin. Intensity data for the crystal were collected using Mo Kα (λ = 0.71073 Å) radiation on a Bruker SMART APEX diffractometer equipped with a CCD area detector at 293 K. The crystallographic data are collected in Table 1. The *SMART*[39] program was used for collecting frames of data, indexing the reflections, and the determination of lattice parameters; the *SAINT*[39] program was used for the integration of the intensity of reflections and scaling; the *SADABS*[40] program was used for absorption correction; and the *SHELXTL*[41] program was used for the space group and structure determination and least-squares refinements on F^2. The structure was solved by the heavy-atom method. Other non-hydrogen atoms were located in successive difference Fourier syntheses. The final refinement was performed by a full-matrix least-squares analysis. Hydrogen atoms attached

(34) Cox, D. D.; Que, L., Jr. *J. Am. Chem. Soc.* **1988**, *110*, 8085−8092.
(35) (a) *Japan Chemical Society, Kagaku-Binran Basic Part II*, 2nd ed.; Maruzen: Tokyo, 1975. (b) Sawyer, D. T. *Oxygen Chemistry*; Oxford University Press: New York, 1991.
(36) Zirong, D.; Battacharya, S.; McCusker, J. M.; Hagen, P. M.; Hendrickson, D. N.; Pierpont, C. G. *Inorg. Chem.* **1992**, *31*, 870−877.
(37) Weiner, H.; Finke, R. G. *J. Am. Chem. Soc.* **1999**, *121*, 9831−9842.
(38) Weiner, H.; Hayashi, Y.; Finke, R. G. *Inorg. Chim. Acta* **1999**, *291*, 426−437.
(39) *SMART and SAINT Software Reference Manuals*, version 5.0; Bruker AXS, Inc.: Madison, WI, 1998.
(40) Sheldrick, G. M. *SADABS Software for Empirical Absorption Correction*; University of Göttingen: Göttingen, Germany, 2000.
(41) *SHELXTL Reference Manual*, version 5.1; Bruker AXS, Inc.: Madison, WI, 1998.

Table 1. Crystal Data and Structure Refinement for **3**

empirical formula	$C_{19}H_{26}Cl_2Fe\ N_3O$
fw	439.18
cryst syst	monoclinic
space group	*C*2/*c*
a (Å)	16.524(4)
b (Å)	7.1673(15)
c (Å)	35.346(7)
β (deg)	103.317(8)
V (Å^3)	4073.6(15)
T (K)	293(2)
Mo Kα λ, (Å)	0.71073
density (Mg m^{-3})	1.432
Z	8
μ (mm^{-1})	1.016
F(000)	1832
no. of reflections collected	9617
GOF on F^2	1.058
R1[a]	0.0652
wR2[b]	0.1310

[a] $R1 = \sum||F_o| - |F_c||/\sum|F_o|$. [b] $wR2 = \sum w[(F_o^2 - F_c^2)^2/\sum w[(F_o^2)^2]\}^{1/2}$.

to the ligand moiety were located from the difference Fourier map and refined isotropically.

Results and Discussion

The ligand *N*,*N*-dimethyl-*N*′-(pyrid-2-ylmethyl)-*N*′-(2-hydroxy-3,5-dimethylbenzyl)ethylenediamine (H(L3)) was synthesized according to a known procedure,[20,34] which involves a simple substitution reaction, with suitable modifications. The stoichiometric reaction of $FeCl_3$ and H(L3) in the presence of Et_3N results in the formation of the complex $[Fe(L3)Cl_2]$ (**3**) in 75% yield. The formulation of the complex is based on elemental analysis and is supported by its X-ray crystal structure. The presence of two cis-coordinated chloride ions in the complex would facilitate the bidentate coordination of the 3,5-di-*tert*-butylcatechol (H_2DBC) to iron(III). The conductivity results reveal quite certainly that only one chloride ion is coordinated in methanol solution (Λ_M, 123 Ω^{-1} cm^2 mol^{-1}). However, both chloride ions are coordinated in acetonitrile (Λ_M, 24 Ω^{-1} cm^2 mol^{-1}) and DMF (Λ_M, 38 Ω^{-1} cm^2 mol^{-1}) solutions. The complex has a magnetic moment of 5.96 μ_B at room temperature, which is characteristic of high-spin iron(III).[18−22,24]

Description of Crystal Structure of $[Fe(L3)Cl_2]$ (3). The molecular structure of complex **3** is shown in Figure 1 together with the atom-numbering scheme, and the selected bond lengths and bond angles are collected in Table 2. The molecule contains a FeN_3OCl_2 coordination sphere with distorted octahedral geometry constituted by the phenolate oxygen atom, the pyridine nitrogen atom and two tertiary amine nitrogen atoms of the tripodal ligand occupying four coordination sites of the octahedron, and two chloride ions occupying the remaining two cis-coordination sites. The 3,5-dimethylphenolate oxygen atom occupies a coordination site trans to the pyridine nitrogen and cis to the sterically hindered $-NMe_2$ group. The chloride ions are located trans to the tertiary amine nitrogens at longer distances. The bond angles of N3−Fe1−Cl1 (170.44°), O1−Fe1−N1 (163.12°), and N2−Fe1−Cl2 (163.21°) deviate markedly from that of an ideal octahedron (180°), suggesting distortion in the octahedral coordination geometry. The Fe−O−C bond angle in **3** (134.0°) is higher than those observed for octahedral iron(III)−phenolate complexes,[18,19] suggesting the importance of the sterically demanding $-NMe_2$ group[20] as in **1**. Interestingly, it is close to that (Fe−O−C, 133° (equatorial), 148° (axial)) of the 3,4-PCD enzyme.[10,15] The higher Fe−O−C bond angles are possibly imposed by the stereochemical constraints of the enzyme and lead to the quite different equatorial and axial Fe−O(tyrosinate) bond distances (1.81 and 1.91 Å), which illustrates the function of the enzyme.[15] The replacement of the electron-withdrawing *p*-nitrophenolate moiety[20] in the analogous complex $[Fe(L1)Cl_2]$ (**1**) by the electron-releasing 3,5-dimethylphenolate moiety (Scheme 2) to obtain **3** leads to the shortening of both $Fe-O_{phenolate}$ (**1**, 1.929 Å; **3**, 1.889 Å) and $Fe-NMe_2$ bonds (**1**, 2.334 Å; **3**, 2.312 Å) with a concomitant increase in $Fe-N_{py}$ (**1**, 2.180 Å; **3**, 2.227 Å) and Fe−Cl (**1**, 2.285 and 2.339 Å; **3**, 2.2999 and 2.3667 Å) bond lengths, with virtually no change in the $Fe-N_{amine}$ bond distance (**1**, 2.213 Å; **3**, 2.214 Å) and a decrease in the Fe−O−C bond angle (**1**, 136.1°; **3**, 134.0°) as well. The Fe−N and Fe−O bond lengths are typical of high-spin octahedral iron(III) complexes.[18−20,22,24,29,42] The shorter Fe−O bond distance in **3** suggests that the iron−oxygen overlap is stronger than that in the analogous complex **1**[20] on account of the more Lewis-basic 3,5-dimethylphenolate donor and that the Lewis acidity of the iron(III) center in **3** is lower. The replacement of the pyridylmethyl arm in

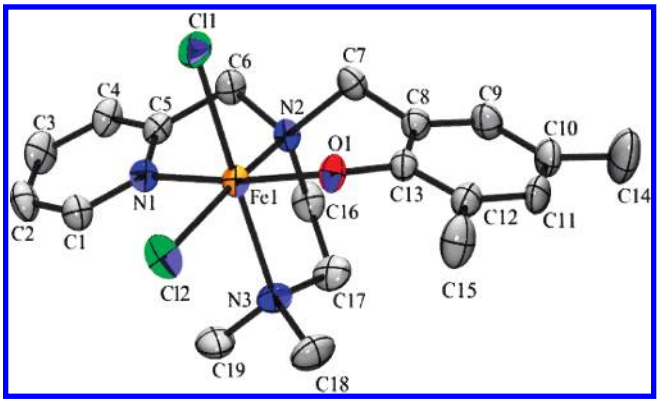

Figure 1. Molecular structure of **3** (40% probability factor for the thermal ellipsoid). Hydrogen atoms have been omitted for clarity.

Table 2. Selected Bond Lengths (Å) and Bond Angles (deg) for **3**

Fe(1)−O(1)	1.889(3)	Fe(1)−N(1)	2.227(4)
Fe(1)−Cl(1)	2.3667(16)	Fe(1)−N(2)	2.214(4)
Fe(1)−Cl(2)	2.2999(16)	Fe(1)−N(3)	2.312(4)
O(1)−Fe(1)−N(2)	88.74(15)	N(1)−Fe(1)−N(3)	87.87(16)
O(1)−Fe(1)−N(1)	163.12(16)	Cl(2)−Fe(1)−N(3)	89.41(12)
N(2)−Fe(1)−N(1)	74.38(15)	O(1)−Fe(1)−Cl(1)	94.85(12)
O(1)−Fe(1)−Cl(2)	103.32(12)	N(2)−Fe(1)−Cl(1)	92.30(12)
N(2)−Fe(1)−Cl(2)	163.21(11)	N(1)−Fe(1)−Cl(1)	85.91(12)
N(1)−Fe(1)−Cl(2)	93.23(12)	Cl(2)−Fe(1)−Cl(1)	98.17(6)
O(1)−Fe(1)−N(3)	89.01(16)	N(3)−Fe(1)−Cl(1)	170.44(12)
N(2)−Fe(1)−N(3)	79.02(16)	C(13)−O(1)−Fe(1)	134.0(3)

(42) (a) Fujii, H.; Funabashi, Y. *Angew. Chem., Int. Ed.* **2002**, *41*, 3638−3641. (b) Kurahashi, T.; Kobayashi, Y.; Nagatomo, S.; Tosha, T.; Kitagawa, T.; Fujii, H. *Inorg. Chem.* **2005**, *44*, 8156−8166. (c) Kurahashi, T.; Oda, K.; Sugimoto, M.; Ogura, T.; Fujii, H. *Inorg. Chem.* **2006**, *45*, 7709−7721.

Scheme 2. Effect of Incorporating Electron-Releasing 3,5-dimethylphenolate Donors on Iron(III) Coordination Geometry, Fe−O Bond Length, and Fe−O−C Bond Angle

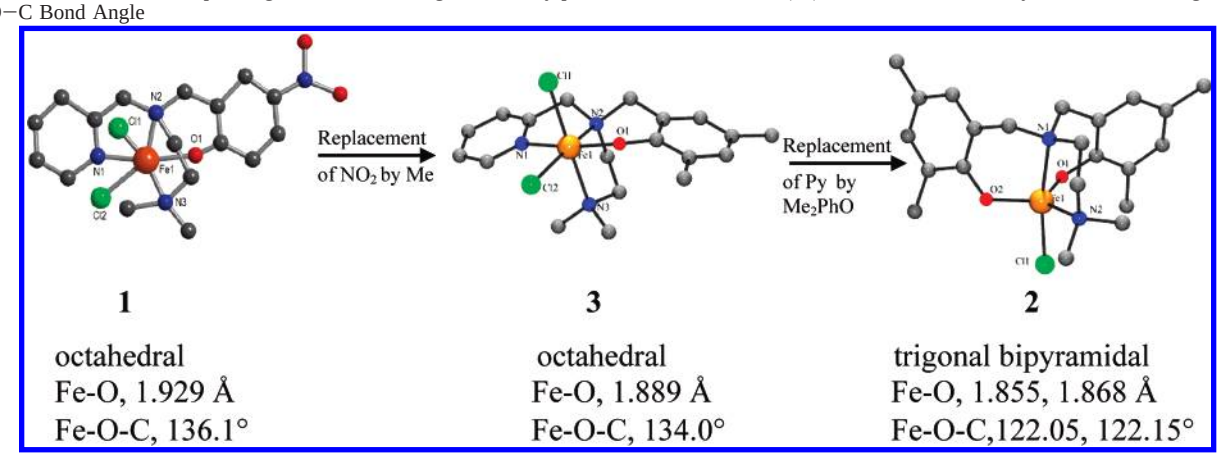

3 by one more electron-releasing 3,5-dimethylphenolate arm (Scheme 2) as in the analogous complex [Fe(L2)Cl] (**2**) confers, interestingly, the unusual trigonal-bipyramidal coordination geometry on iron(III),[19] which closely resembles that of the 3,4-PCD enzyme active site, but with relatively low Fe−O−C bond angles (122.05° and 122.15°). Also, it leads to the shortening of the Fe−$O_{phenolate}$ bond lengths (1.868 and 1.855 Å), which suggests a lower Lewis acidity for iron(III) center in **2**, and a concomitant decrease in Fe−O−C bond angles (122.05° and 122.15°, Supporting Information, Table S1), which are much less than that in **3**, with only one 3,5-dimethylphenolate arm, and also that in **1**. Furthermore, the presence of two 3,5-dimethylphenolate moieties with enhanced Lewis basicity is insufficient, and the presence of the sterically hindering $-NMe_2$ arm is essential to confer a trigonal-bipyramidal coordination geometry on iron(III), emphasizing the importance of steric as well as electronic effects in iron(III) on coordination geometry. Thus, very recently, Fujii et al. have shown[42] that the binding of water as an external ligand to the iron(III) center in a sterically hindered complex leads to a structural change from a preferred square-pyramidal to a distorted trigonal-bipyramidal geometry.

Electronic Absorption and EPR Spectra. In methanol solution, **3** exhibits two bands (Figure 2 and Table 3) around 360 (ϵ, 4690 M^{-1} cm^{-1}) and 650 nm (ϵ, 2390 M^{-1} cm^{-1}),

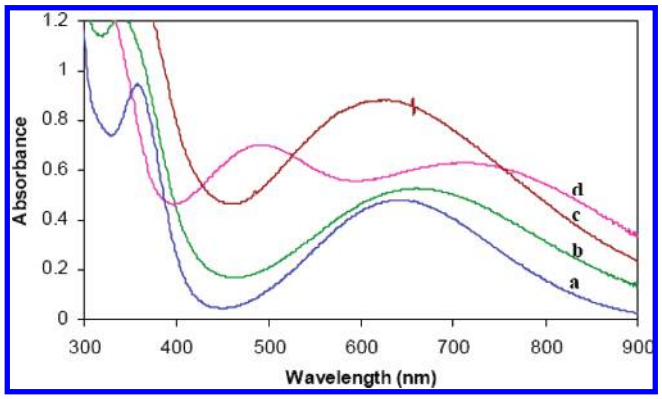

Figure 2. Electronic absorption spectra of **3** (2.0×10^{-4} M) before (a) and after (b) removal of Cl^- ions by adding 2 equiv of $AgNO_3$ and its catecholate adduct generated in situ before (c) and after (d) the removal of Cl^- ion by adding 2 equiv of $AgNO_3$.

Table 3. Electronic Spectral Data[a] for Iron(III) Complexes and Their Adducts in Methanol

	λ_{max}, nm (ϵ, M^{-1} cm^{-1})		
added ligand	$[Fe(L3)Cl_2]$	$[Fe(L3)Cl_2]$[b] + 2 $AgNO_3$	$[Fe(L1)Cl_2]$[c]
none	650 (2390) 361 (4690) 288 (7 220)	665 (2630) 341 (6180) 279 (12 200)	545 (3755) 430 (3195) 360 (17 405) 250 (14 035)
DBC^{2-}	617 (4360) 337 (8050) 280 (14 800) 243 (15 820)	719 (3150) 494 (3510) 288 (17 130)	790 (3260) 485 (3320) 380 (14 770) 295 (8795)
TBC^{2-}	611 (6760) 288 (42 020) 239 (45 460)	667 (2630) 482 (2890) 288 (12 710)	760 (2825) 485 (3375) 370 (14 800) 295 (9345)
CAT^{2-}	564 (5470) 320 (12 520) 283 (29 750) 238 (38 630)	588 (2670) 475 (sh) 286 (14 170)	730 (2670) 480 (3025) 365 (14 695) 295 (8920)
TCC^{2-}	558 (7110) 287 (29 100) 235 (51 340)	569 (3100) 438 (sh) 291 (11 040)	650 (3365) 480 (3755) 355 (15 570) 310 (10 575)
3-$MCAT^{2-}$	569 (6740) 320 (12 760) 285 (37 800) 235 (44 390)	627 (2880) 478 (3370) 286 (13 920)	
4-$MCAT^{2-}$	578 (7320) 323 (13 270) 289 (39 340) 239 (49 490)	674 (2740) 495 (sh) 290 (12 990)	
4-$NCAT^{2-}$	517 (13 600) 399 (35 350) 320 (25 740) 265 (57 820) 236 (55 470)	553 (sh) 398 (9870) 263 (1760)	

[a] Concentration of iron(III) complexes = 2.0×10^{-4} M. The ratio of added ligands to iron(III) complex is 1:1. The catecholate anions were generated by adding 2 equiv of Et_3N. [b] Chloride ions were removed by adding $AgNO_3$. [c] Data taken from ref 20.

which are assigned[17−19,43] respectively to phenolate ($p\pi$) → Fe^{III} ($d\sigma^*$) and phenolate ($p\pi$) → Fe^{III} ($d\pi^*$) LMCT transition, and the ligand-based bands around 288 nm (ϵ, 7220 M^{-1} cm^{-1}). Interestingly, when it is treated with $AgNO_3$ (to remove coordinated chloride ions), the low-energy LMCT band experiences a red shift to 665 nm with an increase in absorptivity (ϵ, 2630 M^{-1} cm^{-1}). This is expected because the removal of the coordinated chloride anions from the iron(III) coordination sphere would decrease the negative

Table 4. Electronic Spectral and Fe^{III}/Fe^{II} Redox Potentials for **3** in Acetonitrile and DMF

solvent	complex	LMCT band λ_{max}, nm (ϵ, M^{-1} cm^{-1})	$E_{1/2}$ (V)[c] CV	$E_{1/2}$ (V)[c] DPV
acetonitrile	$[Fe(L3)Cl_2]$	342 (2750) 618 (1420)	−0.256	−0.257
	$[Fe(L3)Cl_2]$ + DBC^{2-} [a]	480 (2360) 690 (2660)	−0.767	−0.765[d]
	$[Fe(L3)Cl_2]$ + DBC^{2-} [b]	476 (3530) 717 (3700)	-	-
DMF	$[Fe(L3)Cl_2]$	341 (2750) 612 (1420)	−0.604	−0.587
	$[Fe(L3)Cl_2]$ + DBC^{2-} [a]	484 (3520) 694 (3560)	−0.714	−0.718[d]
	$[Fe(L3)Cl_2]$ + DBC^{2-} [b]	473 (3830) 724 (3340)		

[a] DBC^{2-} generated by treating H_2DBC with 2 equiv of triethylamine. [b] DBC^{2-} generated by treating H_2DBC with 2 equiv of piperidine. [c] Scan rate of 50 mV/s (CV) and 1 mV/s (DPV). [d] $Fe^{III} \rightarrow Fe^{II}$ + ligand reduction.

charge built on iron(III) causing the stabilization[18] of the d orbitals and, hence, the decrease of the phenolate-to-iron(III) LMCT band energy. The LMCT band observed around 650 nm in MeOH solution is blue shifted to 618 (ϵ, 1420 M^{-1} cm^{-1}, Table 4) and 612 nm (ϵ, 1420 M^{-1} cm^{-1}) in acetonitrile and DMF solutions, respectively, which is consistent with both the chloride ions of **3** remaining coordinated in solution (cf. above).

When **3** is interacted with a series of catecholate anions generated in methanol solution by treating the catechols with 2 equiv of Et_3N as the base, a new band in the range of 517−617 nm (H_2DBC, 617 nm; ϵ, 4380 M^{-1} cm^{-1}) assignable to the catecholate-to-iron(III) LMCT transition[18−22,24,44] is observed (Figure 2 and Table 3). This is similar to that observed[19] previously for the five-coordinate complex **2** (Supporting Information, Table S1), which shows only one catecholate-to-iron(III) LMCT band, suggesting the monodentate coordination of catecholate ion-to-iron(III) in **3** also. This is in contrast to the observation of two catecholate-to-iron(III) LMCT bands (790, 485 nm) for **1** on treatment with DBC^{2-} (Et_3N) and also for [Fe(HDP)(DBC)] (**4**) (726, 476 nm) (H(HDP) = 2-[(bis(2-pyridylmethyl)-aminomethyl]-4,6-dimethylphenol).[34] The two bands originate from charge transfer from two different catecholate orbitals to iron(III), corresponding to the bidentate coordination[20] of DBC^{2-}, possibly by displacing the two coordinated chloride ions or the weakly coordinated $-NMe_2$ donor (2.334 Å) and one of the coordinated chloride ions in **1**. Interestingly, the catecholate adduct generated in situ by treating **3** with H_2DBC pretreated with 2 equiv of piperidine in methanol solution displays two DBC^{2-}-to-iron(III) LMCT bands around 742 (ϵ, 3510 M^{-1} cm^{-1}) and 483 nm (ϵ, 3710 M^{-1} cm^{-1}). Also, when **3** is treated with $AgNO_3$ (to remove coordinated chloride ions) and then DBC^{2-} (Et_3N), two new DBC^{2-}-to-iron(III) CT bands (719 nm, ϵ, 3150 M^{-1} cm^{-1}; 494 nm, 3510 M^{-1} cm^{-1}, Figure 2 and Table 3) are observed, suggesting the substitution of two solvent molecules (or one solvent molecule and the weakly coordinated $-NMe_2$ group) by chelating DBC^{2-}. This is in sharp contrast to the observation of a single blue-shifted DBC^{2-}-to-iron(III) LMCT band (540−503 nm, Supporting Information, Table S1) when **2** is treated with $AgNO_3$ followed by DBC^{2-} (Et_3N) in the present study. Furthermore, **3** exhibits two catecholate-to-iron(III) LMCT bands in acetonitrile (690 nm, 2660 M^{-1} cm^{-1}; 480 nm, 2360 M^{-1} cm^{-1}) and DMF (694 nm, 3560 M^{-1} cm^{-1}; 484 nm, 3520 M^{-1} cm^{-1}) solutions, suggesting the bidentate coordination of DBC^{2-} (Et_3N) by displacing both the coordinated chloride ions (cf. above, Table 4). Thus, it is clear that the decreased Lewis acidity of the iron(III) center in **3** on account of the coordination of the 3,5-dimethylphenolate donor with enhanced Lewis basicity leads to the displacement of only one of the weakly coordinated chloride ions (cf. conductivity studies) by methanol to form $[Fe(L3)(MeOH)(Cl)]^+$ species. The latter reacts with H_2DBC pretreated with the weaker base Et_3N (pK_a (BH^+) = 10.64) to form [Fe(L3)(HDBC)(Cl)] and with H_2DBC pretreated with a stronger base like piperidine (pK_a (BH^+) = 11.22) to form [Fe(L3)(DBC)]. The monodentate coordination of $HDBC^-$ in the iron(III)[36] and iron(II)[31] complexes has been demonstrated previously by X-ray crystal structures. Upon

$$[Fe(L3)Cl_2] + MeOH \rightleftharpoons [Fe(L3)(MeOH)(Cl)]^+ + Cl^-$$

$$[Fe(L3)(MeOH)(Cl)]^+ + HDBC^- \rightleftharpoons [Fe(L3)(HDBC)(Cl)] + MeOH$$

$$[Fe(L3)(MeOH)(Cl)]^+ + DBC^{2-} \rightleftharpoons [Fe(L3)(DBC)] + Cl^- + MeOH$$

removal of the coordinated chloride in $[Fe(L3)(Cl)(MeOH)]^+$ by treatment with $AgNO_3$, the Lewis acidity of the iron(III) center is enhanced, encouraging the bidentate coordination of DBC^{2-} to form [Fe(L3)(DBC)]. A further decrease in the Lewis acidity of the iron(III) center on moving from **3** to **2** with two 3,5-dimethylphenolate donors of enhanced basicity leads to the reluctance of **2** to expand its coordination sphere. All these observations illustrate the critical role of the Lewis acidity of the iron(III) center, the base used for the deprotonation of H_2DBC, and the solvents in dictating the mode of coordination of DBC^{2-}.

The position of the low-energy catecholate $\rightarrow Fe^{III}$ LMCT band for complex-substrate adducts [Fe(L3)(catecholate)] generated from **3** after removal of coordinated chloride is found to be shifted to higher energies as the substituents[18−22,44] on the catecholate ring are varied from electron-releasing to electron-withdrawing, as observed[20] previously for **1**: DBC^{2-} (719 nm) > 4-$MCAT^{2-}$ (674 nm) > TBC^{2-} (667 nm) > 3-$MCAT^{2-}$ (627 nm) > CAT^{2-} (588 nm) > TCC^{2-} (569

(43) (a) Casella, L.; Gullotti, M.; Pintar, A.; Messouri, L.; Rockenbauer, A.; Gyor, M. *Inorg. Chem.* **1987**, *26*, 1031−1038. (b) Wang, S.; Wang, L.; Wang, X.; Luo, Q. *Inorg. Chim. Acta* **1997**, *254*, 71−77. (c) Krebs, B.; Schepers, K.; Bremer, B.; Henkel, G.; Althus, E.; Muller-Warmuth, W.; Griesar, K.; Haase, W. *Inorg. Chem.* **1996**, *35*, 2360−2368. (d) Gaber, B. P.; Miskowski, V.; Spiro, T. G. *J. Am. Chem. Soc.* **1974**, *96*, 6868. (e) Shongwe, M. S.; Kaschula, C. H.; Adsetts, M. S.; Ainscough, E. W.; Brodie, A. M.; Morris, M. J. *Inorg. Chem.* **2005**, *44*, 3070. (f) Imbert, C.; Hratchian, H. P.; Lanznaster, M.; Heeg, M. J.; Hryhorczuk, L. M.; McGarvey, B. R.; Schlegel, H. B.; Verani, C. *Inorg. Chem.* **2005**, *44*, 7414.

(44) Cox, D. D.; Benkovic, S. J.; Bloom, L. M.; Bradley, F. C.; Nelson, M. J.; Que, L., Jr.; Wallick, D. E. *J. Am. Chem. Soc.* **1988**, *110*, 2026−2032.

nm) > 4-NCAT^{2-} (553 nm). This is expected, as the electron-releasing substituents on the catecholate ring would lower the position, while the electron-withdrawing substituents would raise the position of the low-energy band,[18−22,24] thus reflecting the importance of the electronic effects provided by the substituents on catechols. The order of energy of the catecholate-to-iron(III) LMCT band observed (Table 3) when **3** is treated with various catecholates (Et_3N) to form [Fe(L3)(catecholate)(Cl)], HDBC$^-$ (617 nm) > HTBC$^-$ (611 nm) > H(4-MCAT)$^-$ (578 nm) > H(3-MCAT)$^-$ (569 nm) > HCAT$^-$ (564 nm) > HTCC$^-$ (558 nm) > H(NCAT)$^-$ (517 nm), is almost the same as that observed above for the low-energy band upon bidentate coordination of DBC^{2-} to **3** after the removal of coordinated chloride ions. This implies that the electronic effects in iron(III) in [Fe(L3)(HDBC)(Cl)] are very similar to those in [Fe(L3)(DBC)].

The frozen solution EPR spectrum of **3** (Figure 3 and Supporting Information Table S2) displays high-spin ($S = {}^5/_2$) rhombic ferric signals[42,44] at $g = 8.5$, 4.3, and 2.1 (E/D, 0.088) associated with $|{}^5/_2, -{}^1/_2\rangle \rightarrow |{}^5/_2, +{}^1/_2\rangle$ transition and also signals corresponding to rhombic low-spin[45,46] ($S = {}^1/_2$) iron(III) species ($g = 2.04$, 1.99, 1.87). Upon removal of the coordinated chloride ions by treatment with $AgClO_4 \cdot H_2O$, **3** exhibits similar high-spin ferric signals but with small shifts in g values (8.2, 4.1, 2.2; E/D, 0.086). The small decrease in E/D value reveals a small decrease in rhombicity upon the increase in the Lewis acidity of the iron(III) center on the substitution of chloride ions by solvent molecules. When interacted with DBC^{2-} (Et_3N), **3** exhibits appreciable shifts in g values of the rhombic signals (8.0, 4.1, 2.1; E/D, 0.081) with a decrease in intensity of the low-spin iron(III) signals, and this is consistent with monodentate coordination of catecholate (cf. above). Furthermore, an intense signal appears at $g = 2.03$, which is assignable to low-spin iron(III)-bound semiquinonate species,[46] which has been invoked in both intra- and extradiol-cleavage mechanisms.[13] On the other hand, when DBC^{2-} is added to **3** pretreated with 2 equiv of $AgClO_4 \cdot H_2O$, the high-spin rhombic features are unaffected (8.1, 4.2, 2.15; E/D, 0.081), the signals due to low-spin iron(III) species disappear, and a highly intense semiquinone signal appears at 2.04, suggesting the strong bidentate coordination of DBC^{2-} to form [Fe(L3)(DBC)] adducts. In contrast to **3**, the five-coordinate complex **2** exhibits[19] an intense signal around $g = 5.5$ and a weak signal around 2.0 signifying the absence of any rhombicity in the iron(III) coordination geometry. However, after treatment with $AgClO_4 \cdot H_2O$, **2** exhibits a rhombic EPR spectrum (Supporting Information, Figure S5) with high-spin ferric signals (8.6, 4.2, 2.1; E/D, 0.092) and low-spin iron(III) signals (2.02, 1.95, 1.88). When DBC^{2-} is added to **2** pretreated with $AgClO_4 \cdot H_2O$, no appreciable shift in the rhombic spectral features (8.5, 4.2, 2.11, E/D, 0.090) is observed and, in contrast to **3**, no strong signal around $g = 2.0$ characteristic of semiquinone radical is observed, which is consistent with the inactivity of the complex toward dioxygen. The E/D values of both **2** and its DBC^{2-} adduct are almost the same, suggesting similar five-coordinate geometries for both of them.

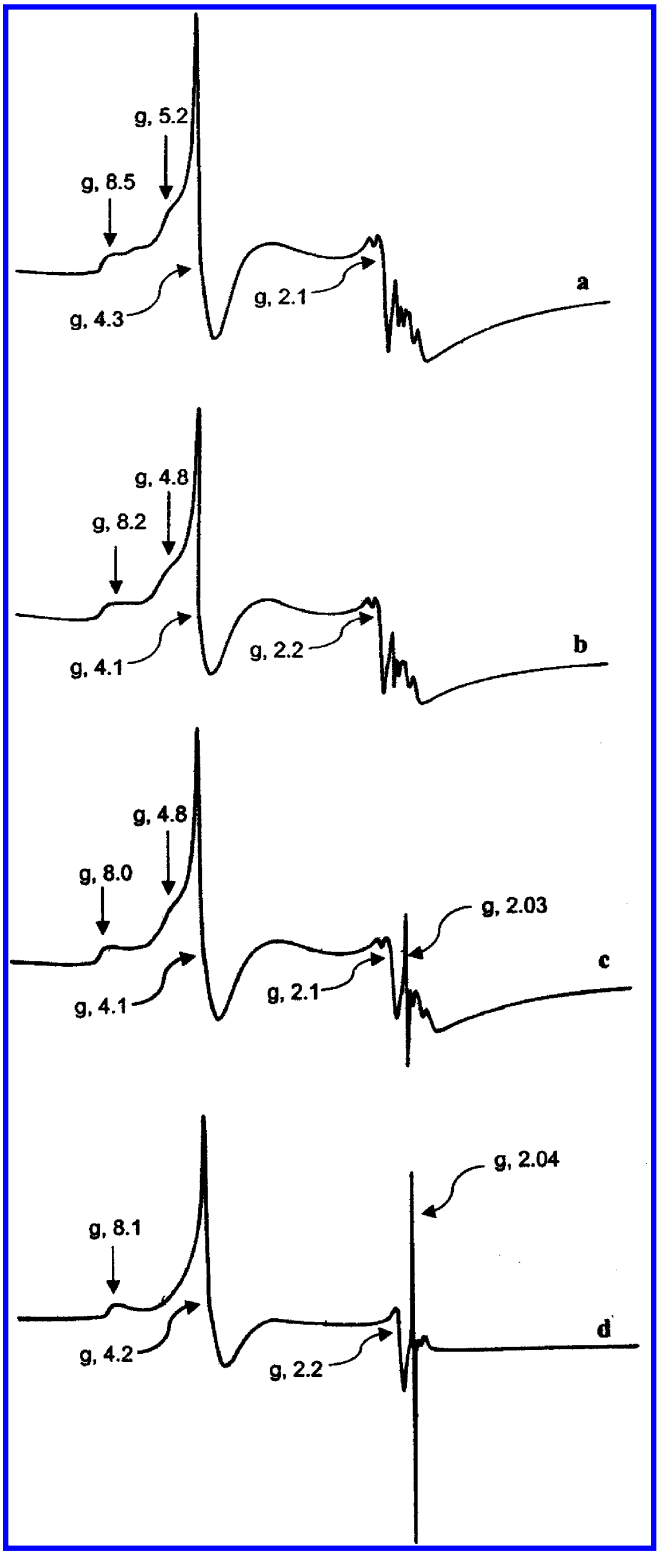

Figure 3. EPR spectra of **3** before (a) and after removal of coordinated chloride ions by adding $AgClO_4 \cdot H_2O$ (b), [Fe(L3)(HDBC)(Cl)] (c), and [Fe(L3)(DBC)] (d) in frozen methanol/acetone solution at 77 K.

Redox Properties. The electrochemical properties of **3** and its H_2DBC adduct generated in situ were studied in

(45) (a) Simaan, A. J.; Biollot, M.-L.; Riviere, E.; Boussac, A.; Girerd, J.-J. *Angew. Chem., Int. Ed.* **2000**, *39*, 196−198. (b) Bukowshi, M. R; Comba, P.; Limberg, C.; Merz, M.; Que. L., Jr.; Wistuba, T. *Angew. Chem., Int. Ed.* **2004**, *43*, 1283−1287.
(46) Yoon, S.; Lee, H.-J. Lee, K.-B.; Jang, H. G. *Bull. Korean Chem. Soc.* **2000**, *21*, 923−928.

Table 5. Electrochemical Data[a] for **3** and Its DBC^{2-} Adduct[c] in Methanol at 25 ± 0.2 °C Using a Scan Rate of 50 mV/s (CV) and 1 mV/s (DPV)

compound	E_{pc} (V)	E_{pa} (V)	ΔE_p (mV)	$E_{1/2}$ (V) CV	$E_{1/2}$ (V) DPV	redox process
$[Fe(L3)Cl_2]$	−0.375	−0.285	90	−0.330	−0.329	$Fe^{III} \rightarrow Fe^{II}$
+ H_2DBC	−0.384	−0.274	110	−0.328	−0.327	$Fe^{III} \rightarrow Fe^{II}$
+ DBC^{2-}	−0.644	−0.534	110	−0.589		$Fe^{III} \rightarrow Fe^{II}$ + ligand reduction
	−0.160	−0.072	88	−0.116	−0.125	$DBSQ \rightarrow H_2DBC$
$[Fe(L3)(MeOH)_2]$[b]	−0.309	−0.257	52	−0.283	−0.276	$Fe^{III} \rightarrow Fe^{II}$
+ H_2DBC	−0.322	−0.280	42	−0.301	−0.283	$Fe^{III} \rightarrow Fe^{II}$
	−0.190	−0.084	106	−0.137	−0.071	$DBSQ \rightarrow H_2DBC$
+ DBC^{2-}					−0.629	$Fe^{III} \rightarrow Fe^{II}$ + ligand reduction
	−0.040				−0.083	$DBSQ \rightarrow H_2DBC$
	0.162				0.623	$DBQ \rightarrow DBSQ$

[a] Potential measured vs $Ag/AgNO_3$ (0.01 M, 0.1 M TBAP); add 0.544 V to convert to NHE. [b] Chloride ions removed by adding $AgClO_4 \cdot H_2O$. [c] Generated by adding 1 equiv of H_2DBC and 2 equiv of triethylamine to complex **3**.

methanol solution by CV and DPV. The complex shows both cathodic and anodic waves ($E_{1/2,}$ − 0.329 V, Supporting Information Figures S2 and S3 and Table 5). The value of the diffusion coefficient (D, 1.1×10^{-6} cm^2/s) calculated by substituting the slope obtained from the linear i_{pc} vs $\nu^{1/2}$ ($\nu < 0.05$ V s^{-1}) plot in the Randles−Sevcik equation[47] is of the same order as those observed previously[18−21] for a one-electron reduction process in similar[20] iron(III) complexes. The i_{pc} vs $\nu^{1/2}$ plot is linear, but the values of peak current ratio i_{pa}/i_{pc} (0.75) and peak potential separation ΔE_p (90 mV) suggest a fairly reversible to irreversible redox process. On removing the coordinated chloride ions by treating the complex **3** with $AgClO_4 \cdot H_2O$, the Fe^{III}/Fe^{II} redox potential is shifted to a more positive value ($E_{1/2}$, −0.276 V), which is expected[18−21] of the increase in Lewis acidity of the ferric center upon replacing the coordinated chloride by solvent molecules. On replacing the *p*-nitrophenolate arm in **1** by the electron-releasing 3,5-dimethylphenolate arm, as in **3**, the Fe^{III}/Fe^{II} redox potential is shifted to a more negative value (**1**, −0.266; **3**, −0.329 V) suggesting a decreased Lewis acidity of the iron(III) center in **3**, which is consistent with the shorter Fe−O bond in **3** (cf. above). It may be noted that the Fe^{III}/Fe^{II} redox potential of **3** is shifted to a more negative value ($E_{1/2}$, −0.587 V, Table 4) in DMF solution and to a more positive value ($E_{1/2}$, −0.257 V, Table 4) in acetonitrile solution, illustrating the effect of solvent.

On adding 1 equiv of H_2DBC to **3** in methanol solution, no appreciable shift in the redox wave is observed (Figure 4 and Table 5). However, on adding 2 equiv of Et_3N, a new redox wave appears ($E_{1/2}$, −0.125 V), corresponding to the DBSQ/H_2DBC couple.[18−21] The $Fe^{III} \rightarrow Fe^{II}$ reduction process, which is expected[19,20] to be shifted to more negative potentials on incorporating two catecholate hydroxyl groups in the coordination sphere, is difficult to discern, as it would have merged with the ligand reduction waves (−0.589 V). The redox potential of the DBSQ/H_2DBC couple[48] of coordinated $HDBC^-$ observed at −0.125 V is less negative than that of the free DBSQ/H_2DBC couple (E_{pc}, −1.34 V vs SCE)[48], suggesting the stabilization of the coordinated $HDBC^-$ anion. Upon the addition of 1 equiv of H_2DBC to

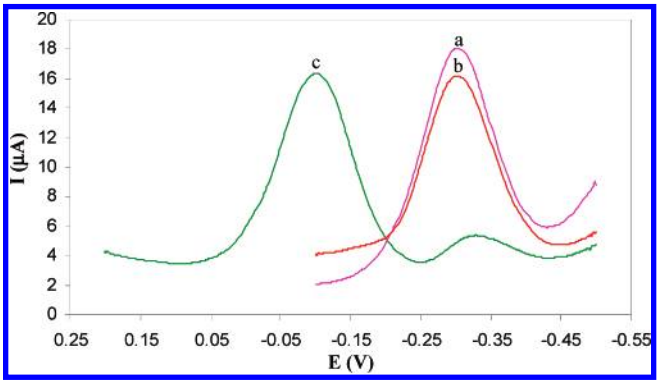

Figure 4. Differential pulse voltammograms of 1 mM **3** before (a) and after the addition of 1 mM H_2DBC (b) and 2 mM Et_3N (c) in methanol at 25 °C. Conditions: supporting electrolyte, 0.1 M TBAP; scan rate, 1 mV s^{-1}; reference electrode, Ag/Ag^+; working electrode, Pt sphere.

3 after treatment with $AgClO_4 \cdot H_2O$ to remove the coordinated Cl^- ions, the reduction current of the $Fe^{III} \rightarrow Fe^{II}$ process ($E_{1/2}$, −0.276 V) decreases and a new redox wave corresponding to the DBSQ/H_2DBC couple ($E_{1/2,}$ −0.071 V, Supporting Information Figure S4 and Table 5) is observed. Further, on adding 2 equiv of Et_3N, the reduction current of the DBSQ/H_2DBC couple ($E_{1/2,}$ −0.083 V, Supporting Information, Figure S4) increases, with the $Fe^{III} \rightarrow Fe^{II}$ reduction wave disappearing and possibly merging with the ligand reduction responses (−0.629 V). The appearance of the DBSQ/H_2DBC redox wave even in the absence of added base is on account of the higher Lewis acidity of the iron(III) center on removing the coordinated chloride ions. Furthermore, the appearance of the DBSQ/H_2DBC couple for [Fe(L3)(DBC)] at a potential (−0.083 V) more positive than that (−0.125 V) for [Fe(L3)(HDBC)(Cl)] reveals that DBC^{2-} coordinated in a bidentate mode in the former is stabilized toward oxidation more than $HDBC^-$, which is coordinated in a monodentate fashion. In other words, the higher Lewis acidity of the iron(III) center in $[Fe(L3)(MeOH)_2]^{2+}$ enhances the covalency of the iron−catecholate interaction and increases the semiquinone character of the bound DBC^{2-}.

Kinetics and Reactivity Studies. The oxygenation reactions of the complex-H_2DBC adducts prepared in situ (using Et_3N or piperidine as base) were investigated in various solvents. When a methanolic solution of the substrate adduct [Fe(L3)(HDBC)(Cl)], generated in situ by reacting **3** with H_2DBC pretreated with 2 equiv of Et_3N (cf. above), is

(47) Bard, A. J.; Faulkner, L. R. *Electrochemical Methods: Fundamentals and Applications;* John Wiley & Sons: New York, 1980; pp 218.
(48) Nanni, E. J.; Stalling, M. D.; Sawyer, D. T. *J. Am. Chem. Soc.* **1980**, *102*, 4481−4485.

Table 6. Kinetic Data for the Oxidative Cleavage of H_2DBC Catalyzed by **3** in Different Solvents and the Cleavage Products Analyzed after 24 h (see Scheme 3)

		Cleavage products (%)[b]				
complex	solvent/base	intradiol	extradiol	k_{obs} (10^{-5} s^{-1})	k_{O_2} (10^{-2} M^{-1} s^{-1})[c]	$t_{1/2}$ (h)[d]
[Fe(L3)(HDBC)(Cl)]	CH_3OH/Et_3N	0.5 (**6**)	17.3 (**9**, **10**, **13**)[e]	1.19 ± 0.21	0.56 ± 0.01	16.1
[Fe(L3)(DBC)]	CH_3OH/Pip	22 (**5**, **6**, **7**)	42 (**9**, **10**, **11**)	4.29 ± 0.56	2.02 ± 0.03	4.5
[Fe(L3)(DBC)][a]	CH_3OH/Pip	56 (**7**)	30 (**9**, **11**)	135.97 ± 1.62	64.14 ± 0.76	0.1
[Fe(L3)(DBC)]	CH_3CN/Pip	40 (**7**)	<1 (**11**, **12**)	8.07 ± 0.84	1.00 ± 0.10	2.4
	CH_3CN/Et_3N			8.84 ± 0.45	1.09 ± 0.06	2.2
[Fe(L3)(DBC)]	DMF/ Pip	94 (**7**, **8**)	<1 (**11**, **12**)	19.34 ± 1.27	3.98 ± 0.26	1.0
	DMF/Et_3N			6.36 ± 0.36	1.31 ± 0.07	3.0

[a] $[Fe(L3)(MeOH)_2]^{2+}$ species generated from $[Fe(L3)Cl_2]$ by adding 2 equiv of $AgNO_3$. [b] Based on H_2DBC, piperidine (Pip). [c] $k_{O_2} = k_{obs}/[O_2]$. [d] $t_{1/2} = 0.693/k_{obs}$. [e] 48 h.

Scheme 3. Cleavage Products of H_2DBC Catalyzed by Complex **3** in the Presence of O_2

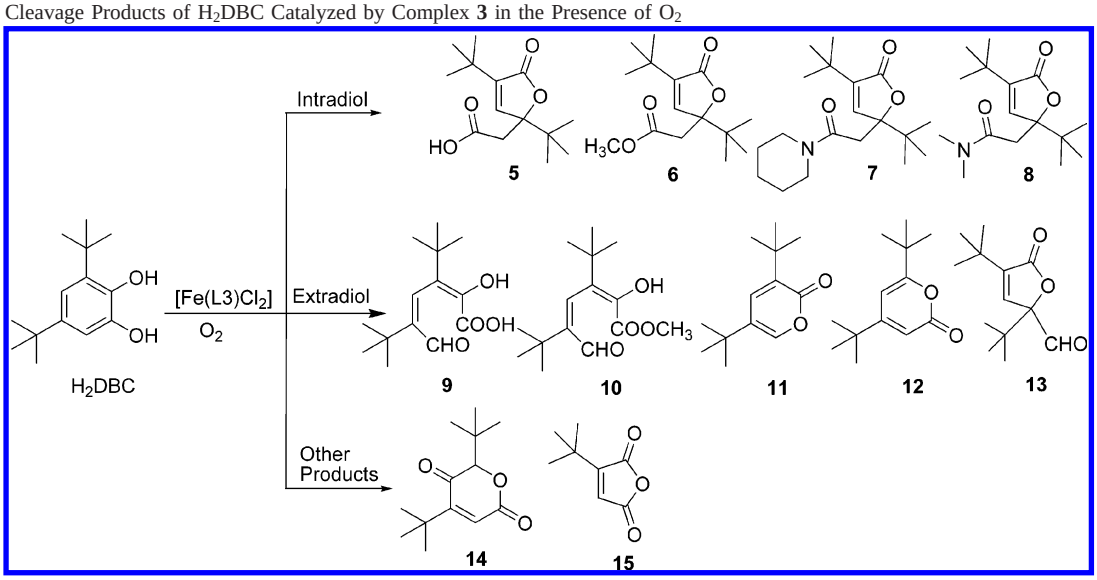

exposed to O_2, the absorbance of the $HDBC^-$-to-iron(III) LMCT band (λ_{max}, 617 nm; ϵ, 4360 M^{-1} cm^{-1}) decreases very slowly (Supporting Information, Figure S6) with pseudo-first-order kinetics due to an excess of dioxygen. The electronic spectrum of the reaction mixture after 96 h shows the disappearance of the 617 and 339 nm bands and the appearance of bands around 568 (ϵ, 5020 M^{-1} cm^{-1}) and 326 nm (ϵ, 14 890 M^{-1} cm^{-1}) indicating the completion of the oxygenation reaction. The rate constant (k_{obs}, 1.19×10^{-5} s^{-1}, Table 6) was calculated by fitting the decrease in intensity of the band into the following equation[49] applicable for relatively slow reactions

$$A = A_\infty + (A_0 - A_\infty)\exp(-k_{obs}t) \qquad (1)$$

where t is time, A, A_0, and A_∞ are the absorbances at time t, 0 and ∞, respectively, and k_{obs} is the pseudo-first-order rate constant. The second-order rate constant k_{O_2} ($= k_{obs}/[O_2]$) was then calculated[18−22,50,51] as 5.6×10^{-3} M^{-1} s^{-1}. The complex [Fe(L3)(HDBC)(Cl)] was reacted with dioxygen over 48 h ($t_{1/2}$, 16.1 h) to afford almost exclusively extradiol (17.3%) and a trace amount (0.5%) of intradiol products (Scheme 3and Table 6). The oxygenation products were identified by GC-MS (EI) and ^{1}H NMR and quantified by GC (FID) techniques. The extradiol ring-cleavage products[26,32,37,38] $C_{14}H_{20}O_4$, *m*/*z* 252, *cis*,*cis*-3,5-di-*tert*-butyl-2-hydroxymuconic semialdehyde (**9**) (15%), $C_{14}H_{22}O_5$, *m*/*z* 268, 3,5-di-*tert*-butyl-2-hydroxymuconic semialdehyde methyl ester (**10**) (1.1%), and 3,5-di-*tert*-butyl-5-(formyl)-2-furanone (**13**) (1.2%) and the intradiol-cleavage product $C_{15}H_{24}O_4$, *m*/*z* 268, (2,4-di-*tert*-butyl-5-oxo-2,5-dihydrofuran-2-yl)acetic acid methyl ester (**6**) (0.5%), are formed. Similar very slow rate of cleavage and lower cleavage yield for [Fe(TACN)(Cat)(Cl)] when Et_3N was used as an external base have been noted by Bugg et al.[32] Molecular oxygen replaces the coordinated chloride ion in [Fe(L3)(HDBC)Cl], and on activation it attacks the semiquinone form of $HDBC^-$ coordinated to iron(III) in a monodentate fashion.

The reactivity of the adduct [Fe(L3)(DBC)] generated in situ in methanol solution by treating **3** with H_2DBC pretreated with 2 equiv of piperidine was determined by monitoring the decay of the DBC^{2-}-to-iron(III) LMCT band around 742 nm on exposure to an excess of dioxygen (Supporting Information, Figure S7). The decay of the band is faster than that for the complex species [Fe(L3)(HDBC)(Cl)] in methanol (cf. above). The second-order rate constant (k_{O_2}, 2.0×10^{-2} M^{-1} s^{-1}) for the reaction was calculated using eq 1.

(49) Hitomi, Y.; Yoshida, M.; Higuchi, M.; Minami, H.; Tanaka, T.; Funabiki, T. *J. Inorg. Biochem.* **2005**, *99*, 755−763.
(50) (a) Mialane, P.; Tehertanov, L.; Banse, F.; Sainton, J.; Girerd, J. *Inorg. Chem.* **2000**, *39*, 2440−2444.
(51) Yamahara, R.; Ogo, S.; Watanabe, Y.; Funabiki, T.; Jitsukawa, K.; Masuda, H.; Einaga, H. *Inorg. Chim. Acta* **2000**, *300*−*302*, 587−596.

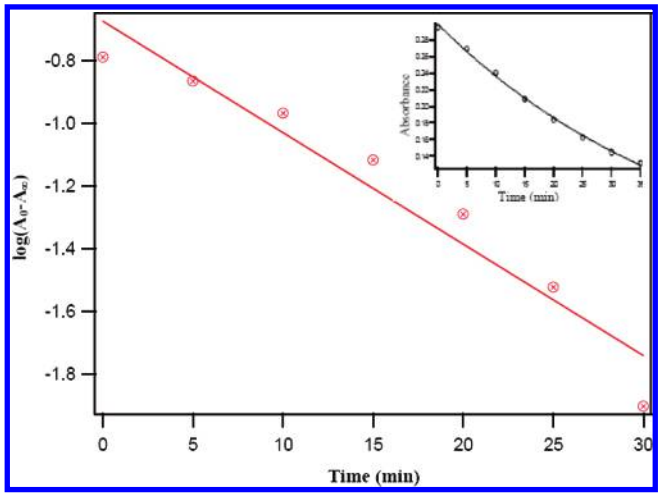

Figure 5. Plot of $\log(A_0 - A_\infty)$ vs time observed at 719 nm (R^2, 0.93) for the reaction of [Fe(L3)(DBC)] (generated in situ after the removal of chloride ions from $[Fe(L3)Cl_2]$ by adding 2 equiv of $AgNO_3$) with O_2 at 25 °C in methanol solution. Concentration: [Fe(L3)(DBC)] = 1.0×10^{-4} M. Inset: progress of reaction.

Upon exposure of the adduct [Fe(L3)(DBC)] to an excess of dioxygen over 24 h ($t_{1/2}$, 4.5 h) in methanol, major amounts of extradiol products (42%) [Scheme 3 and Table 6, **9** (33%) and **10** (2%), both obtained by extradiol ring fission,[26,32,33,37,38] and $C_{13}H_{20}O_2$, *m*/*z* 208, 3,5-di-*tert*-butyl-2-pyrone (**11**) (7%) with the insertion of an oxygen atom into H_2DBC followed by the loss[26,29] of CO], lower amounts of intradiol[16,20,21] products (22%) [$C_{14}H_{20}O_4$, *m*/*z* 254, 3,5-di-*tert*-butyl-5-(carboxymethyl)-2-furanone (**5**) (10%), **6** (3%), and $C_{19}H_{31}NO_3$, *m*/*z* 321, 3,5-di-*tert*-butyl-5-(2-oxo-2-piperidinylethyl)-5*H*-furanone (**7**) (trace)], and $C_{13}H_{19}O_3$, *m*/*z* 223, 2,5-di-*tert*-butyl-2*H*-pyran-3,6-dione (**14**) (5%) and $C_8H_{10}O_3$, *m*/*z* 154, 3-*tert*-butylfuran-2,5-dione (**15**) (4%) as side products[16,20,21] were obtained. It is clear that the bidentate coordination of catechol (cf. above) favors intradiol-cleavage products via the substrate activation mechanism.[13,17] Also, the weakly coordinated $-NMe_2$ (2.312 Å, cf. above) group in [Fe(L3)(DBC)] is displaced to facilitate dioxygen binding,[31] and the bound dioxygen then attacks the semiquinone form of the catechol, which is coordinated in a monodentate fashion, leading to extradiol cleavage.[28,32,33] As the bidentate coordination of DBC^{2-} by displacement of the coordinated methanol or $-NMe_2$ group will be inhibited by electron-releasing 3,5-Me_2 substituents on the phenolate ring in [Fe(L3)(DBC)], lower yields of intradiol-cleavage products are obtained.

The adduct [Fe(L3)(DBC)] generated in situ by treating **3** with $AgNO_3$ and then DBC^{2-} (Et_3N) in methanol solution displays the immediate decay of the DBC^{2-}-to-iron(III) LMCT band at 719 nm (cf. above) on exposure to an excess of dioxygen (Figure 5), and the second-order rate constant (k_{O_2}, 6.4×10^{-1} M^{-1} s^{-1}) was calculated by using eq 1. The product analysis after 24 h of reaction ($t_{1/2}$, 0.14 h) using piperidine as the base reveals an increase in the yield of the intradiol product **7** (56%) and a decrease in the yield of the extradiol-cleavage products **9** (30%) and **11** (2%). Furthermore, the adduct generated in DMF and CH_3CN in situ by treating **3** with DBC^{2-} (piperidine) (DMF, 724 nm; CH_3CN, 717 nm, Table 4) undergoes slower oxygenation on exposure to excess of dioxygen (Supporting Information, Figure S8), and the rate constants were calculated as above (k_{O_2} = (DMF) 4.0×10^{-2} and (CH_3CN) 1.0×10^{-3} M^{-1} s^{-1}). The analysis of cleavage products after 24 h of reaction ($t_{1/2}$ = (DMF) 1.0 and (CH_3CN) 2.4 h) reveals that intradiol cleavage is favored with an exclusive (DMF, 92%) or higher amount of the intradiol-cleavage products **7** (CH_3CN, 40%) and 3,5-di-*tert*-butyl-5-(*N*,*N*-dimethylamidomethyl)-2-furanone (**8**) (DMF, 1.7%), traces of the extradiol-cleavage products **11** (<1%) and 4,6-di-*tert*-butyl-2-pyrone **12** (<1%) (Table 6), and **14** (DMF, 1.3%; CH_3CN, 2.8%) as side product. As illustrated above, the bidentate coordination of catechol in [Fe(L3)(DBC)] favors intradiol-cleavage products via a substrate activation mechanism.[13,17] Also, the solvent molecules can displace the weakly coordinated $-NMe_2$ (2.312 Å, cf. above) group but may in turn be difficult to be displaced by dioxygen for extradiol cleavage to occur.

It is interesting to note that the rate of cleavage for [Fe(L3)(HDBC)(Cl)] (k_{O_2} = 5.6×10^{-3} M^{-1} s^{-1}) to afford exclusively extradiol product is almost four times slower than that (k_{O_2} = 2.0×10^{-2} M^{-1} s^{-1}) for [Fe(L3)(DBC)] in the same solvent (methanol) to yield both intra- and extradiol products. This illustrates the importance of the base used to deprotonate the catechol substrate and the slowness of the extradiol-cleavage reaction due to the difficulty in generating a vacant coordination site on the iron(III) center and the presence of the iron(III) rather than the iron(II) oxidation state as in the extradiol-cleaving enzyme. Similarly, the inactivity of **2** toward catechol cleavage may be explained on the basis of steric hindrance from the coordinated $-NMe_2$ group and the decreased Lewis acidity of the iron(III) center leading to the monodentate coordination of the substrate ($HDBC^-$) by replacing the axially coordinated chloride ion. It is obvious that the bidentate coordination of DBC^{2-} would require structural changes from trigonal-bipyramidal[19] to octahedral geometry, which is more difficult to achieve than simple substitution reactions in octahedral complexes like **1** and **3**. So, we speculate that the $-NMe_2$ arm in **3** is displaced to create a vacant site, which is susceptible to attack by O_2, as suggested previously.[31] No such vacant site is available for **2**, illustrating its inactivity toward dioxygen activation. The rate of cleavage (k_{O_2} = 6.4×10^{-1} M^{-1} s^{-1}) for [Fe(L3)(DBC)], generated in methanol using Et_3N as the base after the removal of the coordinated chloride ion, to yield increased intra- and decreased extradiol products, is 32 times faster than that for the same complex [Fe(L3)(DBC)] generated by piperidine in the presence of chloride ions. It is clear that the chloride anions compete for the coordination sites of the catecholate adduct. Also, the rate of catechol cleavage for [Fe(L3)(DBC)] in methanol is 130 times faster than that for [Fe(HDP)(DBC)] (**4**) (k_{O_2} = 4.9×10^{-3} M^{-1} s^{-1})[34], with only one iron−phenolate bond, as in [Fe(L3)(DBC)]. On replacing one of the pyridyl moieties in the latter by the $-NMe_2$ pendant to obtain the former, the sterically hindering and weakly coordinated $-NMe_2$ donor enhances the Lewis acidity of iron(III) center and, hence, the binding affinity of DBC^{2-}, leading to the enhanced reaction rate. Also, the

ligand steric hindrance in [Fe(L3)(DBC)] would facilitate the release of products from the reactive intermediate[18−21] and hence the cleavage. Furthermore, the high Lewis acidity of the iron(III) center in [Fe(L3)(DBC)] would enhance the semiquinone character of the bound DBC^{2-} (cf. above) and render the adduct more prone to oxygen attack, thereby accelerating the rate of oxidative cleavage.[13] In nonaqueous solvents, piperidine acts as a base to deprotonate H_2DBC much better than Et_3N, facilitating the bidentate coordination of the catecholate anion and, hence, the faster substrate activation by molecular oxygen to yield intradiol-cleavage products.

Conclusions

The iron(III) complex of a tripodal monophenolate ligand also containing pyridylmethyl and sterically hindered $-NMe_2$ arms possesses a distorted octahedral coordination geometry. On account of the sterically demanding $-NMe_2$ group and the electron-releasing 3,5-dimethylphenolate pendant in the complex, the monoanion $HDBC^-$ of the substrate H_2DBC (3,5-di-*tert*-butylcatechol), generated with 2 equiv of Et_3N as the base, interacts with the complex in a monodentate fashion despite the presence of two cis-coordinated chloride ions. On the other hand, interestingly, the removal of the coordinated chloride ions or the use of a stronger baselike piperidine results in the bidentate coordination of the DBC^{2-}-to-iron(III) center, as revealed by the presence of two DBC^{2-}-to-iron(III) LMCT bands and the observation of the DBSQ/H_2DBC couple at a more positive potential, which is facilitated by the enhanced Lewis acidity of the iron(III) center. Remarkably, for the chloride complex [Fe(L3)Cl_2], the extradiol cleavage of H_2DBC treated with Et_3N base provides an almost exclusively *cis,cis*-3,5-di-*tert*-butyl-2-hydroxymuconic semialdehyde rather than 3,5-di-*tert*-butyl-2-pyranone. However, on removing the coordinated chloride ion or using piperidine as the base, a major amount of intradiol-cleavage product is observed, with considerable enhancement in the cleavage rate. Thus, the cleavage activities of the model complex depend strongly upon the solvent, the base used to deprotonate the substrate, and the mode of coordination—mono- or bidentate—of the catecholate substrate to the iron(III) center, the Lewis acidity of which is tuned by a novel combination of ligand donors. Attempts are in progress to tune the environment around the iron(III) atom by using various sterically hindering donor atoms to enhance the yield of regioselective extradiol cleavage.

Acknowledgment. We sincerely thank the Department of Science and Technology, New Delhi, for supporting this research (Scheme No. SR/S1/IC-45/2003), and the Council of Scientific and Industrial Research, New Delhi, for a Senior Research Fellowship to R.M. We thank Professor P. Sambasiva Rao, Pondicherry University, for providing the EPR facility.

Supporting Information Available: Electronic spectra, EPR spectra and data, cyclic voltammograms, differential pulse voltammograms, and crystallographic data in CIF format for **3**. This material is available free of charge via the Internet at http://pubs/acs.org.

IC700646M